Journal Name

ARTICLE TYPE

Cite this: DOI: 10.1039/xxxxxxxxxx

Investigation of the terahertz vibrational modes of ZIF-8 and ZIF-90 with terahertz time-domain spectroscopy

Nicholas Y. Tan,[a] Michael T. Ruggiero,[b], Claudia Orellana-Tavra,[a] Tian Tian,[a] Andrew D. Bond,[c] Timothy M. Korter,[b] David Fairen-Jimenez,[a] and J. Axel Zeitler*[a]

Received Date
Accepted Date

DOI: 10.1039/xxxxxxxxxx

www.rsc.org/journalname

We present experimental and computational evidence that gate-opening modes for zeolitic imidazole frameworks can be observed at terahertz frequencies. Our work highlights the critical importance to correctly optimise the crystal structure prior to computational lattice dynamics analysis. The results support the hypothesis that the low energy vibrational modes do indeed play a significant role in host-guest interactions for ZIFs, such as gas loading.

Zeolitic imidazolate frameworks (ZIFs) are a subclass of the metal-organic framework (MOF) family which comprise tetrahedral metal centres bridged by imidazolate linkers with topologies similar to zeolites.[1,2] In order to tune the properties of ZIFs, the metal cations can be varied between Zn^{2+}, Li^{+} and B^{3+}, while various functional groups can be added on the imidazolate linkers.[1,3,4] Due to their relatively high thermal and chemical stability, ZIFs have been heavily studied for applications in gas storage,[5] separations,[6] and catalysis.[7] While ZIFs are crystalline solids, some of them (e.g. ZIF-4, ZIF-7 and ZIF-8) have flexible molecular structures which lead to concerted 'swing' motions of the imidazole linkers and changes in the windows or cage structures.[8–11] This has been associated with changes in the accessibility of the pores, making these motions crucial to the molecular adsorption properties of these ZIFs. However, despite the important applications of ZIFs, the fundamental lattice dynamics of these structures have not been fully revealed.

A recent study combined the use of computational methods, inelastic neutron scattering and infra-red spectroscopy to study the lattice dynamics of several different ZIFs.[12] The terahertz frequency region was marked as an area of great interest as *ab initio* quantum mechanical calculations predicted a number soft modes, pore breathing, and gate-opening motions for ZIF-4, ZIF-7 and ZIF-8 falling in the frequency region below 3 THz. Inelastic neutron scattering experiments were performed to probe the terahertz modes of these ZIFs. However, while the experimental spectra matched qualitatively with the simulated spectra in the crucial < 3 THz region, there was insufficient resolution of the spectral features at these frequencies to match conclusively the experimental and simulated spectra. Furthermore, the density functional theory (DFT) simulations of ZIF-8 in the aforementioned study were performed using an imposed reduced crystalline symmetry structure due to the occurrence of imaginary modes in the vibrational calculation. While this method apparently yielded an accurate simulation in the mid-IR region, there is evidence that the simulations deviate from experiment below 3 THz.

Terahertz time-domain spectroscopy (THz-TDS) has been used extensively to study the chemical and structural properties of a variety of systems,[13] ranging from molecular crystals,[14,15] to amorphous solids,[16,17] liquids[18,19] and proteins.[20] It has shown sufficient spectral resolution to differentiate between crystalline polymorphs, as well as probe phase transitions in disordered crystals, and study dynamics in amorphous solids. Due to the non-destructive nature of the technique, spectra across a wide range of temperatures can be readily acquired, allowing for temperature-induced changes in spectral response to be investigated. Given the initial suggestions that swing and gate-opening motions in ZIFs fall within the terahertz frequency region,[12] THz-TDS is used here to probe the terahertz vibrational modes of two ZIFs with the sodalite (SOD) structure: ZIF-8 and ZIF-90. These two systems are particularly interesting due to the swing effect that occurs during the adsorption of small molecules at low and medium relative pressures, respectively, and the opening of the narrow windows around 3.4 Å diameter. The fundamental understanding of flexibility of MOFs is key for the application of these materi-

[a] *Department of Chemical Engineering and Biotechnology, University of Cambridge, Pembroke Street, Cambridge CB2 3RA, U.K.; Tel: +44 1223 334783; E-mail: jaz22@cam.ac.uk*

[b] *Department of Chemistry, Syracuse University, 111 College Place, Syracuse, New York, U.S.A.*

[c] *Department of Chemistry, University of Cambridge, Lensfield Road, Cambridge CB2 1EW, U.K.*

† Electronic Supplementary Information (ESI) available: Characterisation of the materials using X-ray powder diffraction. See DOI: 10.1039/b000000x/

als in industrial separation. We then performed revised *ab initio* quantum mechanical calculations for comparison with the experimental data.

ZIF-8 and ZIF-90 were prepared using previously reported methods.[21,22] 15-60 mg of the respective ZIF sample was mixed with 360 mg of high-density polyethylene and compressed under 2 tons of force for 3 minutes to form approximately 3 mm thick pellets of 13 mm diameter for the THz-TDS measurements. Variable temperature THz-TDS measurements were performed using previously employed equipment and methodology in the range of 0.2 to 2.4 THz (60 mg sample)[23] and using an Advantest TAS7500TS in the range 0.5 to 4.5 THz (15 mg sample). Solid-state DFT calculations were performed using the CRYSTAL14[24] software package, which makes use of periodic boundary conditions to replicate the crystalline nature of the studied materials. The recently implemented M06-2X meta-hybrid exchange correlation functional,[25] designed for use with transition metal containing systems, was coupled with the split-valence double-zeta 6-31G(d,p) basis set[26] for all calculations. Vibrational normal mode eigenvectors and eigenvalues were determined numerically within the harmonic approximation based on fully geometry optimised solids.[27,28] Infrared intensities were calculated using the Berry Phase method.[29]

The terahertz spectrum of ZIF-8 at 90 K shows a weak feature at 1.51 THz, a strong feature at 1.95 THz, several weak features between 2.5 THz and 3.3 THz, as well as a very strong feature at 3.9 THz (Fig. 1a‡); while the spectrum of ZIF-90 at 80 K shows weak and spectrally poorly resolved features at 0.76 and 2.34 THz, and a feature developing at 2.47 THz (Fig. 1b). The simulated spectrum of ZIF-8, which was calculated from the optimised cubic structure ($a = 17.038$ Å), is an excellent match to the experimental spectrum. It is important to note that unlike the previous simulations, the result shown here was optimised within the experimentally determined space group[8,30] (cubic *I-43m*) and did not produce any imaginary frequencies. The literature structure of ZIF-90 exhibits significant disorder and geometrical distortion on account of the imposed *I-43m* crystallographic symmetry. To produce a chemically feasible model, the published structure was expanded to space group *P*1, and the duplicate atoms of the aldehyde groups were deleted. The structure optimised without constraints resulted in a final monoclinic structure in space group $P2_1$ with symmetrised unit-cell parameters $a = 17.612$ Å, $b = 17.256$ Å, $c = 16.923$ Å, $\beta = 90.046°$, $V = 5143.395$ Å^3. The distortions from numerous higher-symmetry space groups are slight, which suggests that the material could adopt a complex domain-type structure.

Analysis of the predicted terahertz vibrational modes in both ZIF-8 and ZIF-90 show that they mostly involve shearing and torsional motions of the imidazolate linkers, and not the rotational motions required for gate opening. However, the strong vibrational mode predicted for ZIF-8 at 1.89 THz, as well as the vibrational modes at 1.13 and 1.31 THz predicted for ZIF-90 result from rotational motions of the linkers, which suggests that they could be the crucial gate-opening motions. The motion of the predicted mode at 3.82 THz in ZIF-8 is primarily a bending of the two imidizolate ligands about the metal coordination bond, which ultimately results in a breathing-type mode of the MOF cavity.

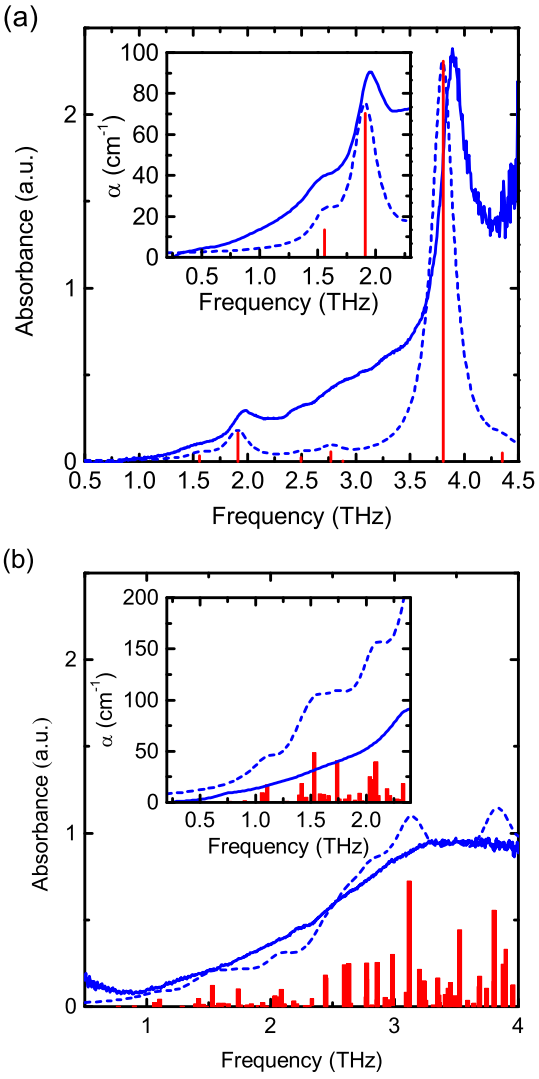

Fig. 1 Experimental and simulated terahertz spectra of (a) ZIF-8 (at 90 K) and (b) ZIF-90 (at 80 K). Solid lines represent experimental spectra and dashed lines represent simulated spectra. Red bars indicate frequencies and intensities of the individual calculated terahertz modes.

Powder X-ray diffraction (PXRD) was carried out on ZIF-8 and ZIF-90 to confirm their structures. The PXRD pattern for ZIF-8 matched well with the published structure[31,32] under both ambient conditions and when the sample was placed under vacuum at 298 K. The PXRD pattern for ZIF-90 under ambient conditions is similar to that of ZIF-8, but the Bragg peaks show different relative intensities. The differences are not attributable to any preferred orientation effect, since they were reproducible between several samples, and furthermore, become similar to those seen in ZIF-8 (ESI,† Fig. S1) when the sample is placed under vacuum.

‡ The spectra in the respective inset plots were acquired from a pellet prepared from 60 mg pure sample using our custom build THz-TDS setup while the main plots were measured after diluting the sample in PE using the commercial terahertz spectrometer.

This suggests that there may be some guest loading in ZIF-90 under ambient conditions. It has been found that water uptake in ZIF-90 is over 30 times higher than that in ZIF-8 at water activities above 0.413 due to the adsorption site in the aldehyde group from the imidazole ring compared to the 2-methylimidazole from ZIF-8.[33] A coarse model with water introduced into the voids in the ZIF-90 structure reproduced this change in Bragg intensities (see ESI† and Fig. S2 and S3), and hence, it is foreseeable that water molecules are adsorbed in ZIF-90 under ambient conditions.

Variable temperature THz-TDS measurements were performed on ZIF-90 in order to investigate further the possibility of guest loading. Below 220 K, minor variations in the spectra are observed. However, the terahertz absorption across the entire frequency range probed increases significantly between 220 and 250 K. Above 250 K, the terahertz absorption then decreases, returning to the original level at 280 K and beyond (Fig. 2). This trend is consistently seen when the measurements are repeated on the same sample.

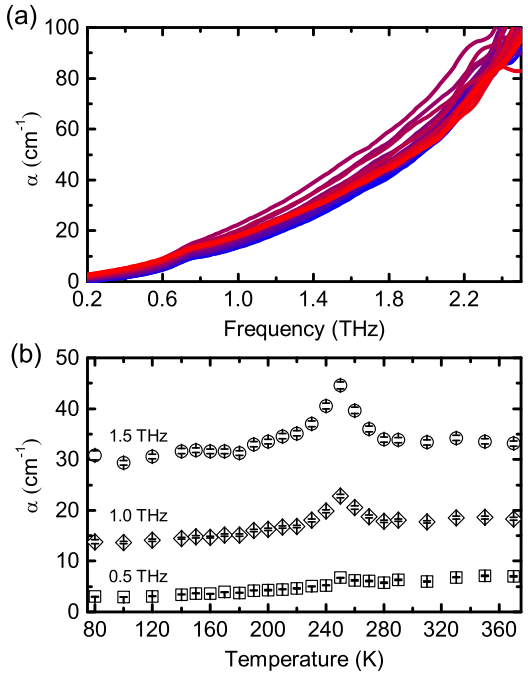

Fig. 2 (a) Terahertz spectra of ZIF-90 from 80 (blue) – 370 (red) K. (b) Terahertz absorption coefficients at 0.5 (squares), 1.0 (diamonds) and 1.5 (circles) THz. Error bars indicate standard deviation over 3 experimental runs.

Given the affinity of ZIF-90 for water, it is possible that some residual water molecules are present in the pores, which freeze when cooled rapidly to 80 K prior to the acquisition of the spectra. Liquid water has very strong terahertz absorption which increases monotonously with frequency. However, crystalline ice has much weaker terahertz absorption, with negligible absorption below 1 THz and small but increasing absorption above 1.3 THz due to a phonon mode centred at 3 THz.[34,35] As the temperature is raised above 220 K, it is possible that the ice begins to melt to give liquid water and this causes the increase in terahertz absorption which is more significant at higher frequencies. Although this is lower than the expected melting point of water, previous reports have found that confinement of organic molecules in porous materials result in melting point depression[36] and changes in the physical state[37] due to the interaction of adsorbates with the microporosity.[38] Above 250 K, the drop in absorption coefficient can be attributed to the evaporation of the liquid water from the pores under prolonged exposure to vacuum conditions which are applied during the variable temperature THz-TDS measurements. This would be consistent with the changes in Bragg intensities seen in the PXRD data at 298 K when placed under vacuum. The absorption returns to the same levels as those below 200 K since ice has negligible contributions to the terahertz absorption, so the ice-loaded and empty ZIF-90 should have similar absorption levels. The fact that this trend can be reproduced multiple times with the same sample suggests that some adsorption of water in ZIF-90 occurs spontaneously under ambient conditions.

In the sample of ZIF-8 we observed that the strong vibrational feature that is observed around 2 THz appears very broad and low in intensity in the spectrum at 80 K. Upon heating to 90 K it red-shifts to slightly lower frequency and sharpens up (Fig. 3). The red-shift ceases at around 120 K and the feature shifts to slightly higher frequencies upon further heating (see inset in Fig. 3). The very strong mode at just below 4 THz appears unaffected by the change in temperature between 80 and 90 K. We cannot explain this behaviour comprehensively at this point but speculate that the change in vibrational features might be indicative of a change in disorder in the structure of ZIF-8 that is associated with the vibrational mode around 2 THz. Further work is required to better understand this behaviour.

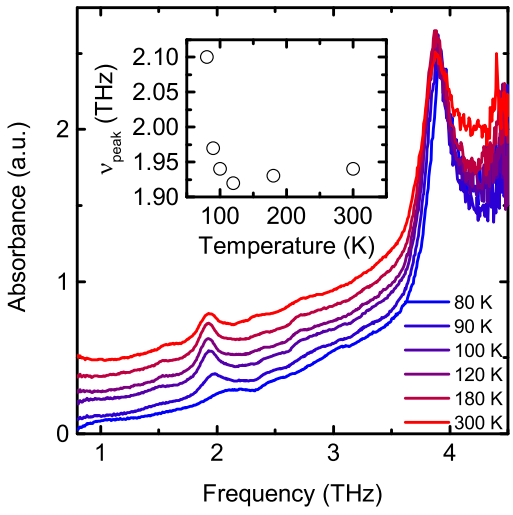

Fig. 3 Experimental spectra of ZIF-8 acquired at temperatures between 80 and 300 K. Spectra are offset by 0.1 a.u. with increasing temperature from 80 K (bottom) to 300 K (top).

In this paper, the terahertz spectrum of ZIF-8 is investigated with a combination of THz-TDS and *ab initio* quantum mechanical calculations. The use of THz-TDS allows for a well resolved spectrum to be obtained, while revised quantum mechanical calculations proved to be an excellent match for the experimental

data. These methods were then extended to ZIF-90 and a reasonable match was also obtained between the experimental and calculated spectra. Closer analysis shows terahertz vibrational modes at 1.89 THz in ZIF-8 and 1.13 and 1.31 THz in ZIF-90 which involve rotational motions of the imidazolate linkers and hence may be the key gate-opening, swing effect motions in these systems. Subsequent PXRD experiments found unusual behaviour in ZIF-90 which could be related to guest loading under ambient conditions. Variable temperature THz-TDS spectra showed significant differences in the 220-280 K temperature range. The spike in absorption and subsequent decrease to the original levels suggest the presence of adsorbed water in ZIF-90 stored under ambient conditions, which is first frozen as ice, then liquefies and subsequently vaporises.

These results demonstrate the utility of THz-TDS in the study of ZIFs and provide further evidence that the crucial gate-opening vibrations in ZIFs lie at terahertz frequencies. Furthermore, variable temperature THz-TDS is shown to be sensitive to host-guest interactions in ZIFs. This demonstrates the potential of the technique in studying such interactions in ZIFs, which will have direct applications in gas and drug loading in these systems.

Acknowledgements

C.O.T. thanks Becas Chile and the Cambridge Trust for funding; D.F.-J. thanks the Royal Society (U.K.) for funding through a University Research Fellowship. T.M.K. would like to acknowledge the Royal Society as well as the Royal Society of Chemistry for support.

Notes and references

1 K. S. Park, Z. Ni, A. P. Côté, J. Y. Choi, R. Huang, F. J. Uribe-Romo, H. K. Chae, M. O'Keeffe and O. M. Yaghi, *Proceedings of the National Academy of Sciences of the United States of America*, 2006, **103**, 10186–10191.
2 X. C. Huang, Y. Y. Lin, J.-P. Zhang and X.-M. Chen, *Angewandte Chemie International Edition*, 2006, **45**, 1557–1559.
3 J. Zhang, T. Wu, C. Zhou, S. Chen, P. Feng and X. Bu, *Angewandte Chemie International Edition*, 2009, **48**, 2542–2545.
4 T. Wu, J. Zhang, C. Zhou, L. Wang, X. Bu and P. Feng, *J. Am. Chem. Soc.*, 2009, **131**, 6111–6113.
5 A. Phan, C. J. Doonan, F. J. Uribe-Romo, C. B. Knobler, M. O'Keeffe and O. M. Yaghi, *Accounts of Chemical Research*, 2009, **43**, 58–67.
6 K. Li, D. H. Olson, J. Seidel, T. J. Emge, H. Gong, H. Zeng and J. Li, *J. Am. Chem. Soc.*, 2009, **131**, 10368–10369.
7 H.-L. Jiang, B. Liu, T. Akita, M. Haruta, H. Sakurai and Q. Xu, *J. Am. Chem. Soc.*, 2009, **131**, 11302–11303.
8 D. Fairen-Jimenez, S. A. Moggach, M. T. Wharmby, P. A. Wright, S. Parsons and T. Düren, *J. Am. Chem. Soc.*, 2011, **133**, 8900–8902.
9 C. Gücüyener, J. van den Bergh, J. Gascon and F. Kapteijn, *J. Am. Chem. Soc.*, 2010, **132**, 17704–17706.
10 D. Fairen-Jimenez, R. Galvelis, A. Torrisi, A. D. Gellan, M. T. Wharmby, P. A. Wright, C. Mellot-Draznieks and T. Düren, *Journal of Materials Chemistry*, 2012, **41**, 10752–10762.
11 M. T. Wharmby, S. Henke, T. D. Bennett, S. R. Bajpe, I. Schwedler, S. P. Thompson, F. Gozzo, P. Simoncic, C. Mellot-Draznieks, H. Tao, Y. Yue and A. K. Cheetham, *Angewandte Chemie International Edition*, 2015, **54**, 6447–6451.
12 M. R. Ryder, B. Civalleri, T. D. Bennett, S. Henke, S. Rudic, G. Cinque, F. Fernandez-Alonso and J.-C. Tan, *Phys. Rev. Lett.*, 2014, **113**, 215502.
13 E. P. J. Parrott and J. A. Zeitler, *Appl Spectrosc*, 2015, **69**, 1–25.
14 J. Sibik, M. J. Sargent, M. Franklin and J. A. Zeitler, *Mol. Pharmaceutics*, 2014, **11**, 1326–1334.
15 E. P. J. Parrott, N. Y. Tan, R. Hu, J. A. Zeitler, B. Z. Tang and E. Pickwell-MacPherson, *Mater. Horiz.*, 2014, **1**, 251.
16 J. Sibik, E. Y. Shalaev and J. A. Zeitler, *Phys. Chem. Chem. Phys.*, 2013, **15**, 11931–11942.
17 J. Sibik, S. R. Elliott and J. A. Zeitler, *J. Phys. Chem. Lett.*, 2014, **5**, 1968–1972.
18 R. Li, C. D'Agostino, J. McGregor, M. D. Mantle, J. A. Zeitler and L. F. Gladden, *J. Phys. Chem. B*, 2014, **118**, 10156–10166.
19 N. Y. Tan, R. Li, P. Bräuer, C. D'Agostino, L. F. Gladden and J. A. Zeitler, *Phys. Chem. Chem. Phys.*, 2015, **17**, 5999–6008.
20 S. Ebbinghaus, S. Kim, M. Heyden, X. Yu, U. Heugen, M. Gruebele, D. Leitner and M. Havenith, *Proceedings of the National Academy of Sciences of the United States of America*, 2007, **104**, 20749–20752.
21 F. K. Shieh, S. C. Wang, S. Y. Leo and K. C. W. Wu, *Chemistry - A European Journal*, 2013, **19**, 11139–11142.
22 K. Kida, M. Okita, K. Fujita, S. Tanaka and Y. Miyake, *Crystengcomm*, 2013, **15**, 1794–1801.
23 N. Y. Tan and J. A. Zeitler, *Mol. Pharmaceutics*, 2015, **12**, 810–815.
24 R. Dovesi, R. Orlando, A. Erba, C. M. Zicovich Wilson, B. Civalleri, S. Casassa, L. Maschio, M. Ferrabone, M. De La Pierre, P. D'Arco, Y. Noël, M. Causà, M. Rérat and B. Kirtman, *International Journal of Quantum Chemistry*, 2014, **114**, 1287–1317.
25 Y. Zhao and D. G. Truhlar, *Theor Chem Account*, 2007, **120**, 215–241.
26 P. C. Hariharan and J. A. Pople, *Theoret. Chim. Acta*, 1973, **28**, 213–222.
27 F. Pascale, C. M. Zicovich Wilson, F. López Gejo, B. Civalleri, R. Orlando and R. Dovesi, *Journal of Computational Chemistry*, 2004, **25**, 888–897.
28 C. M. Zicovich Wilson, F. Pascale, C. Roetti, V. R. Saunders, R. Orlando and R. Dovesi, *Journal of Computational Chemistry*, 2004, **25**, 1873–1881.
29 Y. Noel, C. M. Zicovich Wilson, B. Civalleri, P. D'Arco and R. Dovesi, *Physical Review B*, 2001, **65**, 014111.
30 O. Shekhah, R. Swaidan, Y. Belmabkhout, M. du Plessis, T. Jacobs, L. J. Barbour, I. Pinnau and M. Eddaoudi, *Chemical Communications*, 2014, **50**, 2089–2092.
31 H. Bux, F. Liang, Y. Li, J. Cravillon, M. Wiebcke and J. Caro, *J. Am. Chem. Soc.*, 2009, **131**, 16000–16001.
32 H. Bux, C. Chmelik, J. M. van Baten, R. Krishna and J. Caro, *Advanced Materials*, 2010, **22**, 4741–4743.
33 K. Zhang, R. P. Lively, M. E. Dose, A. J. Brown, C. Zhang, J. Chung, S. Nair, W. J. Koros and R. R. Chance, *Chemical Communications*, 2013, **49**, 3245–3247.
34 K. D. Möller and W. G. Rothschild, *Far-infrared spectroscopy*, WILEY-VCH Verlag, 1971.
35 V. I. Gaiduk and D. S. F. Crothers, *Journal of Molecular Liquids*, 2006, **128**, 145–160.
36 C. L. Jackson and G. B. McKenna, *The Journal of Chemical Physics*, 1990, **93**, 9002–9011.
37 D. Fairen-Jimenez, F. Carrasco-Marín, D. Djurado, F. Bley, F. Ehrburger-Dolle and C. Moreno-Castilla, *J. Phys. Chem. B*, 2006, **110**, 8681–8688.
38 D. Fairen-Jimenez, N. A. Seaton and T. Düren, *Langmuir*, 2010, **26**, 14694–14699.